Front. Optoelectron. 2012, 5(4): 371–389
DOI 10.1007/s12200-012-0283-9

REVIEW ARTICLE

Recent progress on tandem structured dye-sensitized solar cells

Dehua XIONG, Wei CHEN (✉)

Michael Grätzel Centre for Mesoscopic Solar Cells, Wuhan National Laboratory for Optoelectronics, College of Optoelectronic Science and Engineering, Huazhong University of Science and Technology, Wuhan 430074, China

Abstract Tandem structured dye-sensitized solar cells (DSSCs) can take full advantage of sunlight, effectively broadening the absorption spectrum of the cell, resulting in a higher open circuit voltage or short circuit current than that of the conventional DSSC with single light absorber. The theoretical maximum efficiency is therefore suggested to be over the Schottky-Queisser limit of 33%. Accordingly, tandem design of DSSC is thought to be a promising way to break the performance bottleneck of DSSC. Besides, the tandem designs also broaden the application diversity of DSSC technology, which will accelerate its scale-up industrial application. In this paper, we have reviewed the recent progress on photo-electrochemical applications associated with kinds of tandem designs of DSSCs, in general, which are divided into three kinds: "n-type DSSC + n-type DSSC," "n-type DSSC + p-type DSSC" and "n-type DSSC + other solar conversion devices." The working principles, advantages and challenges of these tandem structured DSSCs have been discussed. Some possible solutions for further studies have been also pointed out together.

Keywords dye-sensitized solar cells (DSSCs), tandem structure, photo-electrochemical cell

1 Introduction

Since in 1991 Grätzel and coworkers first discovered a very high internal surface area nanostructured TiO_2 semiconductor material could be used in dye-sensitized solar cells (DSSCs) [1], intense research activity has been devoted to DSSCs in the past two decades [2–7]. To address the issues of energy crisis and environmental pollution in the new century, DSSCs have been regarded as one of the most promising third generation photovoltaic devices for harnessing solar energy source, as the solar energy is clean and renewable. Its ecological and low-cost fabrication processes make DSSC attractive and credible alternative to conventional photovoltaic systems [2–7]. The photoactive electrode (such as TiO_2, SnO_2 or ZnO nanostructured electrode) in the typical Grätzel cell has an "n-type behavior," which we suggested could be called "n-type DSSC." Recently, Grätzel and coworkers have achieved a world record efficiency of 12.3% for n-type DSSC based on porphyrin dye sensitized TiO_2 [8].

To further improve the energy conversion efficiency of DSSC up to 15% is of critical importance for the scale-up industrial application of this cheap and friendly environmental photovoltaic technology. The commonly accepted way is to broaden the light utilization range of DSSC, since the incident photon-to-current conversion responses of all of the reported dyes are much shorter than those of ideal absorbers like crystalline silicon or other semiconductors applied in the first or second generations of solar cells. However, due to the fact that intrinsic light absorption characteristics of the organic dyes are different from the inorganic semiconductors, the attempts relying on developing one dye which could harvest the full solar spectral range encounter with great challenges. The "cocktail method," which mixes two dyes simply in one solution for dye uptake on semiconductive electrode, cannot prevent the interactions between the dyes, which generally cannot give rise to higher performance than that of just using the single dyes.

In the past decade, there were many works focus on employing tandem structures to solve the above mentioned problem, in which design, more than one light absorber were collaboratively harvest solar spectrum. These designs include: 1) two different dyes sensitized n-type semiconductive electrodes are tandem positioned, which is termed to be "n-n tandem structured DSSC" [9–27], giving rise to a higher short-circuit photocurrent density (J_{sc}) of the

Received July 1, 2012; accepted August 8, 2012

E-mail: wnlochenwei@hust.edu.cn

completed device if parallel connected or a higher open-circuit photovoltage (V_{oc}) if series connected; 2) one dye sensitized n-type semiconductive electrode series connected with another dye sensitized p-type semiconductive electrode [28–34], which can be called "n-p tandem structured DSSC", can result in a higher photovoltage; 3) dye sensitized solar cell in combination with other types of solar conversion applications [35–39], such as other types of solar cells, photo-electrochemical cell for water splitting device, solar thermoelectric generator, etc. What is more important, in principle, the tandem structured DSSCs can break through the traditional conversion efficiency (Schottky-Queisser) limit of 33% on the solar cell with single light absorber, to be with the highest theoretical efficiency of 43%, which will leave more space to improve the cell efficiency. This paper reviews the recent progress on kinds of tandem structured DSSCs one by one as the category defined above.

2 n-n tandem structured DSSCs

The n-n tandem structured DSSCs can be divided into three different modes of realization, including: 1) two completed cells tandem positioned (top DSSC + bottom DSSC), as illustrated in Fig. 1; 2) different dyes separately positioned at different depth of one integrated film, as illustrated in Fig. 2; 3) two electrodes sensitized with two dyes, with one floating porous electrode set in the middle of the cell, as illustrated in Fig. 3.

In 2004, Shozo and coworkers first reported a tandem structured DSSC based on two completed cells using N719 sensitized the front cell positioned in front of black dye sensitized bottom cell [9]. The electrode of the front cell is generally high transparent, and it is made of small TiO_2 nanoparticles, which allows most of the solar light without absorbing by N719 dye to penetrate through the front cell and to be absorbed by the black dye at the bottom cell (Fig. 1). The tandem structured cell could finally harvest wider solar spectrum more efficiently than each single cell. As a result, the tandem structured cell exhibit a higher J_{sc} if the two cells are parallel-connected or a higher V_{oc} if the two cells are series-connected than each single DSSC. In the first demonstration, Shozo et al. got the series-connected tandem DSSC with J_{sc} of 15.9 $mA \cdot cm^{-2}$ and solar conversion efficiency (η) of 7.6%, which were both higher than that of the single cells.

Depending on different combinations of dyes, especially

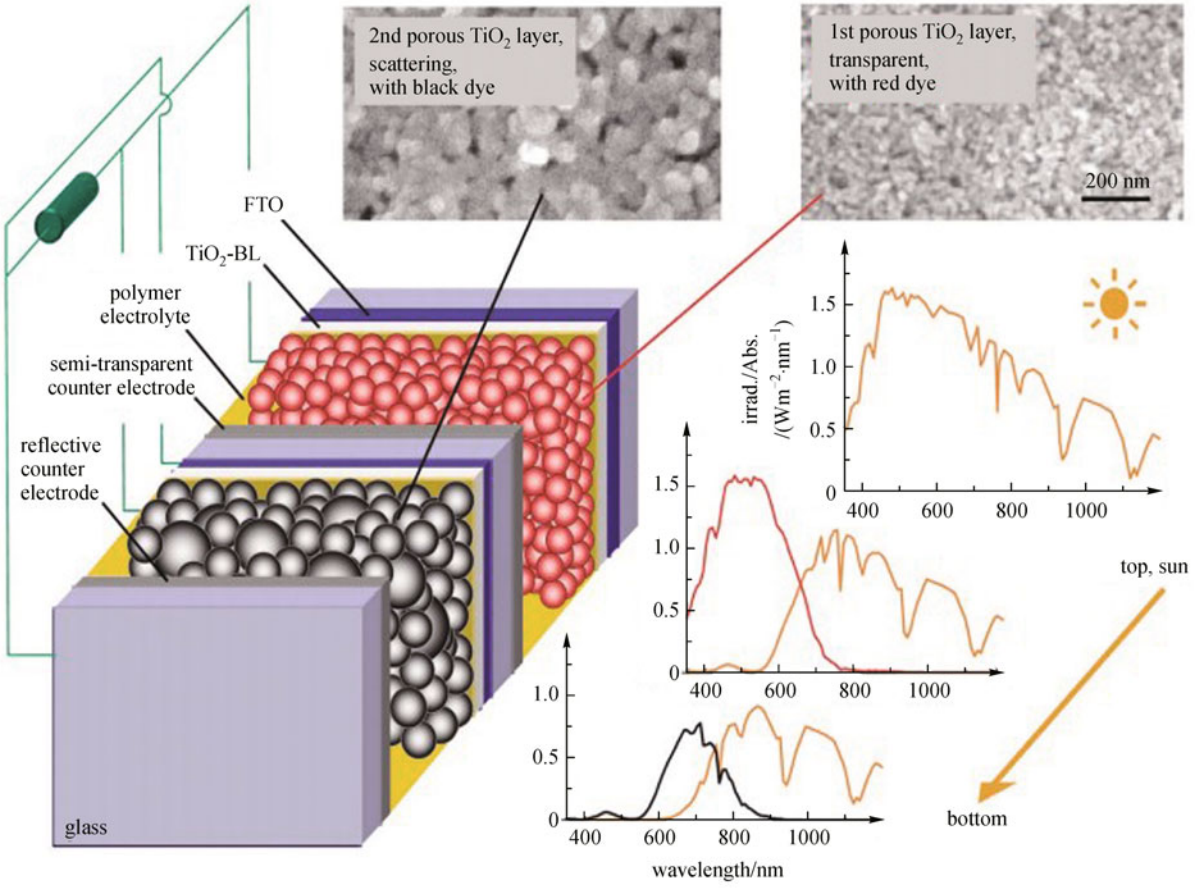

Fig. 1 Schematics of tandem dye-sensitized solar cell made up of two completed cells, scanning electron micrographs, and irradiation spectra (Reprinted with permission from Ref. [10], Copyright (2004), American Institute of Physics)

more efficient near-infrared dyes applied, the tandem design based on two completed cells achieved improved performances. Nelles and coworkers [10] reported that, a η as high as 10.5% and J_{sc} of 21.1 mA·cm^{-2} were achieved for the parallel-connected tandem cell also based on the combination of N719 dye and black dye. It has been demonstrated in their work that J_{sc} of the tandem cell $J_{sc} = J_{sc1} + J_{sc2}$ for the two single cells almost applies. In 2009, Hironori and coworkers reported a series-connected tandem DSSC with optimized dye combination (NKX-2677, N719, NK-6037, and black dye) and TiO_2 electrodes (structure and thickness), and achieved the best performance of V_{oc} of 1450 mV, J_{sc} of 10.8 mA·cm^{-2} and η of 10.4%; V_{oc} of which is consistent with the sum of the V_{oc} of the top and bottom cells [11]. In 2010, Fang and coworkers reported the employment of Li^+-absent electrolyte and/or coating Al_2O_3 on TiO_2 electrode surface in the bottom cell, which resulted in enhanced V_{oc} of the bottom cell and hence that of the tandem cell [12]. Compared to the individual cells (the highest η is 7.58%), the tandem cell with two organic dyes having complementary absorption spectra demonstrates an improved efficiency up to 8.33%. In 2010, Masatoshi and coworkers optimized the thickness of TiO_2 films in the separated cells with respect to the performance of tandem DSSCs with different connection modes (parallel or series). The optimized parallel-connected tandem DSSCs gave the highest η, with the value of 10.6% [13].

The notable feature of the tandem design with two completed cells tandem positioned rests with that: it is easy to fabricate in practice and to achieve a good performance, because the performance for both top cell and bottom cell could be optimized separately. But the drawback is also evident, which mostly rests with the Pt coated counter electrode of the front cell, of which the light absorption cannot be omitted and hence gives rise to a limitation on the overall light harvesting efficiency of the tandem cell. In view of this, Park and coworkers developed a controlled desorption method to position three different dyes in one integrated film, the concept of which is illustrated in Fig. 2. The advantage of this design rests with that the dyes are selectively positioned, which can prevent interactions between each other like what will happen in case of the "cocktail method".

In the first demonstration, Park and coworkers proved that three kinds of dyes with different light absorption range could converse photon to electron cooperatively, the monochromatic incident photon-to-electron conversion efficiency (IPCE) spectrum of the tandem designed cell covers the sum of three dyes' response. J_{sc} of the tandem designed cell is 10.6 mA·cm^{-2}, V_{oc} is 618.6 mV and η is 4.8%. J_{sc} and η are larger than those of each single dye sensitized cells, while V_{oc} is in the middle of that of three single dye sensitized cells; the phenomena are not surprising because the tandem design illustrated in Fig. 2 is theoretically consistent with the series-connected tandem structured DSSC made up of three single cells. Practically, Park's strategy is too complex. They first introduced a polymer to fill in the pore channels of TiO_2 electrode, and therefore desorption rate of the previously absorbed dye in alkaline solution could be controlled. After desorption of one kind dye to a certain depth of TiO_2 film, the TiO_2 electrode was allowed to uptake another dye. At the end of those procedures, the polymers filling in the pore still need to be removed. The complexity of procedure may lead to inadequate dye adsorbing status on TiO_2 surface (the physical position of different dyes might not be strictly separated), which might be the reason why the reported performance of such a tandem designed cell was not so high.

Later in 2011, Ma and coworkers reported a similar tandem designed DSSC with a multilayered photoanode prepared by a simple and low-cost film-transfer technique, as depicted in Fig. 4. The structure of the multilayered

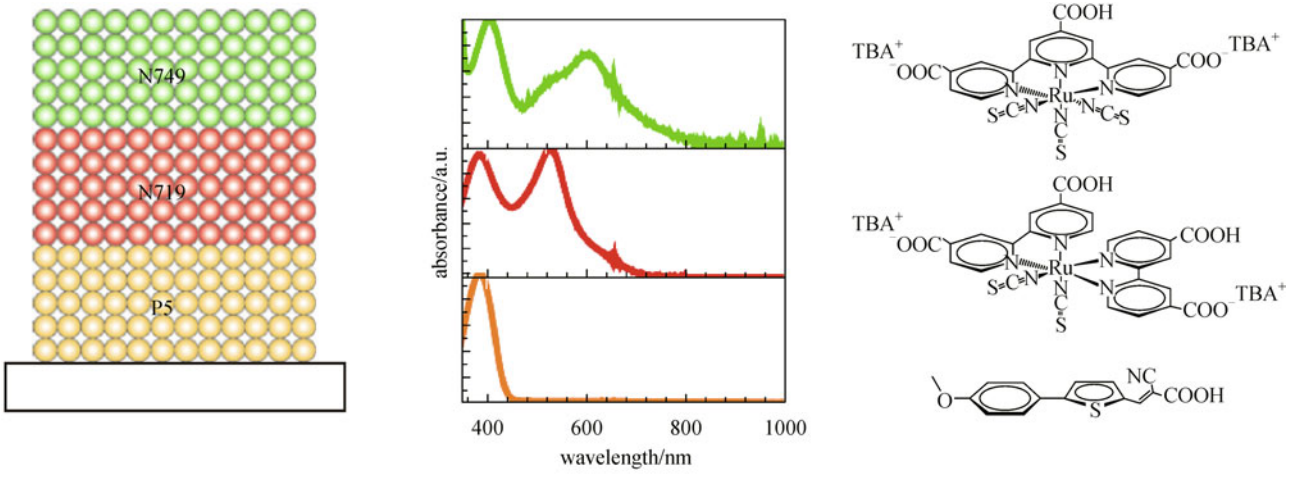

Fig. 2 Selective positioning of different dyes in one integrated film (Reprinted from Ref. [14], Copyright (2009), with permission from Macmillan Publishers Ltd: [Nature Materials])

photoanode consists of TiO_2/dye 1/transferred TiO_2/dye 2. The photocurrent density was significantly enhanced and the highest efficiency of 11.05% was achieved [15]. Nearly at the same time, Cheng and coworkers also reported a similar tandem designed cell, which employed cold-press process to prepare the double layered film on the flexible conducting substrate. As a result, the reported efficiency of the tandem designed flexible DSSC reached a much improved power conversion efficiency of 4.9% [16].

To use available incident light more efficiently, Murayama and coworkers reported a new tandem designed cell structure, of which two dye-sensitized nanocrystalline TiO_2 films were placed face-to-face as working electrodes, and a platinum mesh sheet with suitably high optical transmittance was inserted between the electrodes as a counter electrode [17,18]. The J_{sc} for the tandem cell was found to be equivalent to the sum of the J_{sc} for the front and back photoelectrodes. Under ideal conditions, the total efficiency of the tandem structured DSSC could be improved to be over 10%; it might reach 18% by using the most appropriate design and materials as suggested (if one dye could absorb long wavelength light up to 920 nm). In addition, Shuzi and coworkers reported a similar tandem structured DSSC with one floating porous electrode in the middle (see Fig. 3): the top electrode consists of a transparent TiO_2 film on Fluorine doped Tin Oxide (FTO) sensitized with dye 1 covering a short wavelength region [19], the floating electrode consists of a porous TiO_2 film on stainless mesh sensitized with dye 2. The floating electrode is a self-standing flexible sheet and can be handled easily. Light is introduced from the front side and is absorbed by a top electrode, followed by a bottom electrode. The V_{oc} of the tandem structure DSSC was 0.88 V which was much higher than that of the corresponding single cell (0.6 and 0.66 V) and IPCE curve had two peaks corresponding to those of single cells, but J_{sc} was lower than those of the corresponding single cells.

3 n-p tandem structured DSSCs

In 1999, Lindquist and coworkers reported the first model of dye sensitized p-type NiO based DSSC [20], which we called it "p-type DSSC", as a counterpart of n-type DSSC based on dye sensitized TiO_2. The working principle for p-type DSSC could also refer to that of n-type DSSC. As illustrated in Fig. 5, the only differences rest with that, in p-type DSSC, it is the photon-injected holes diffusing transport in porous p-type semiconductors, and the photon-generated electrons is injected from the dye to the electrolyte to reduce the oxidized iodine species; the theoretical V_{oc} of p-type DSSC is depend on the valence band edge of p-type semiconductor and the redox potential of electrolyte. Therefore, the n-p tandem structured DSSC could result in a higher V_{oc}, theoretically depending on the potential difference between the conduction band edge of TiO_2 and the valence band edge of p-type semiconductor. Furthermore, the n-p tandem design is superior to the above-discussed n-n tandem design, due to omitting the expensive Pt counter electrode and the complexity of cell structure.

In theory, p-type DSSC should be able to work as

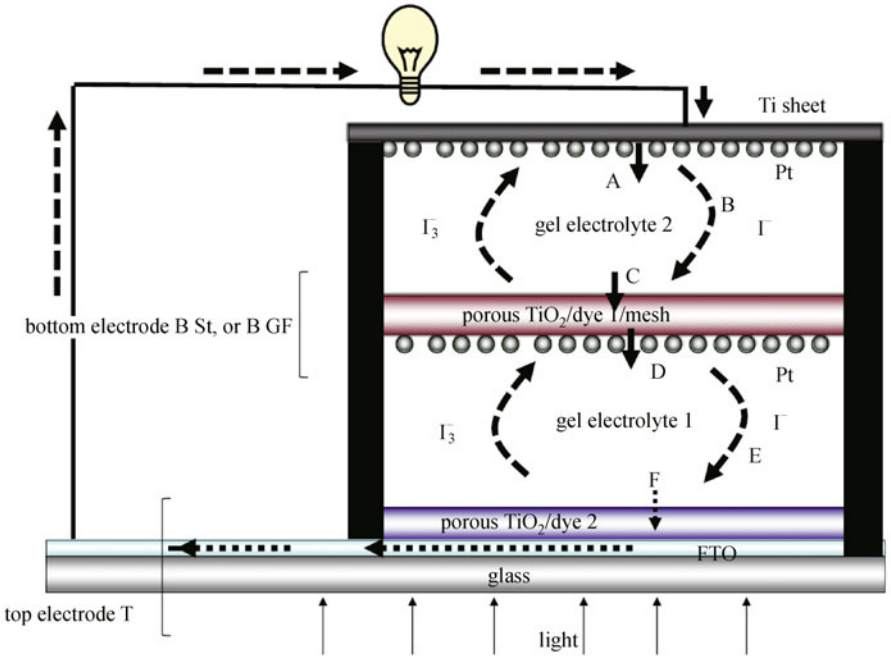

Fig. 3 Structure of tandem cell with one floating porous electrode in the middle (Reprinted with permission from Ref. [19], Copyright (2010), Elsevier)

efficiently as the n-type DSSC. However, most of the p-type DSSCs were reported with poor performances (see Table 1), the highest efficiency was only 0.46%, which was reported by Bach and coworkers [21]. In contrast to n-type DSSC, the p-type DSSC is of a late start and insufficiently studied in the past decade. To further improve the performance of p-type DSSC is of critical importance for the performance improvement on the n-p tandem structured DSSC. It is of no doubt the optimization on p-type DSSC is a systematic work, which should take into account of all of the key components in p-type DSSC, including p-type semiconductors, new dyes adapt for p-type semiconductor and the electrolytes, which will be discussed in latter sections stepwise.

3.1 p-type semiconductors

Just like TiO_2 was found in kinds of n-type semiconductors for highly efficient n-type DSSC, a suitable choice on the p-type semiconductor may have a decisive impact on the performance of p-type DSSC. In p-type DSSC, the photocathode based on nanostructured p-type semiconductor plays several important roles: 1) as a support for dye adsorption; 2) as a hole transport path for hole collection. The candidates of p-type semiconductors should meet the following requirements: wide band gap, large surface area, high surface chemical affinity and suitable valence band potential [5–7]. There are a few metal oxides which exhibit p-type semiconductivity, including NiO [20–39], $CuAlO_2$ [40], and $CuGaO_2$ [41,42], diamond [43], CuO [44], and p-GaP [45], applied in p-type DSSCs so far. NiO was the most frequently reported one, because NiO is a p-type semiconductor with wide bandgap (E_g = 3.6–4.0 eV), good thermal and chemical stability. Furthermore, the valence band edge is positioned at 0.52 V vs NHE, deeper than that of the redox potential of iodine based electrolyte, which allows it to generate a V_{oc} with field direction opposite to that of n-type DSSC [20].

The first work on NiO based p-type DSSC was done by Lindquist and coworkers in 1999, in which, nickel-containing compound slurry was coated on a conductive glass first, and the nanoporous NiO electrodes were obtained after the high-temperature calcination in air [20]. In the later reports, NiO slurries or pastes were prepared by sol-gel [20,22], hydrothermal synthesis [25,28], and electrode position [46,47] method, based on which, the NiO nanoporous films were fabricated by the doctor blade or screen printing method, and then sintering at high temperature (350°C–500°C). With respect to the film thickness of hole transport photocathode, it is generally optimized at about 2 μm, much thinner than 10 μm of TiO_2 photoanode, at which the n-type DSSC can

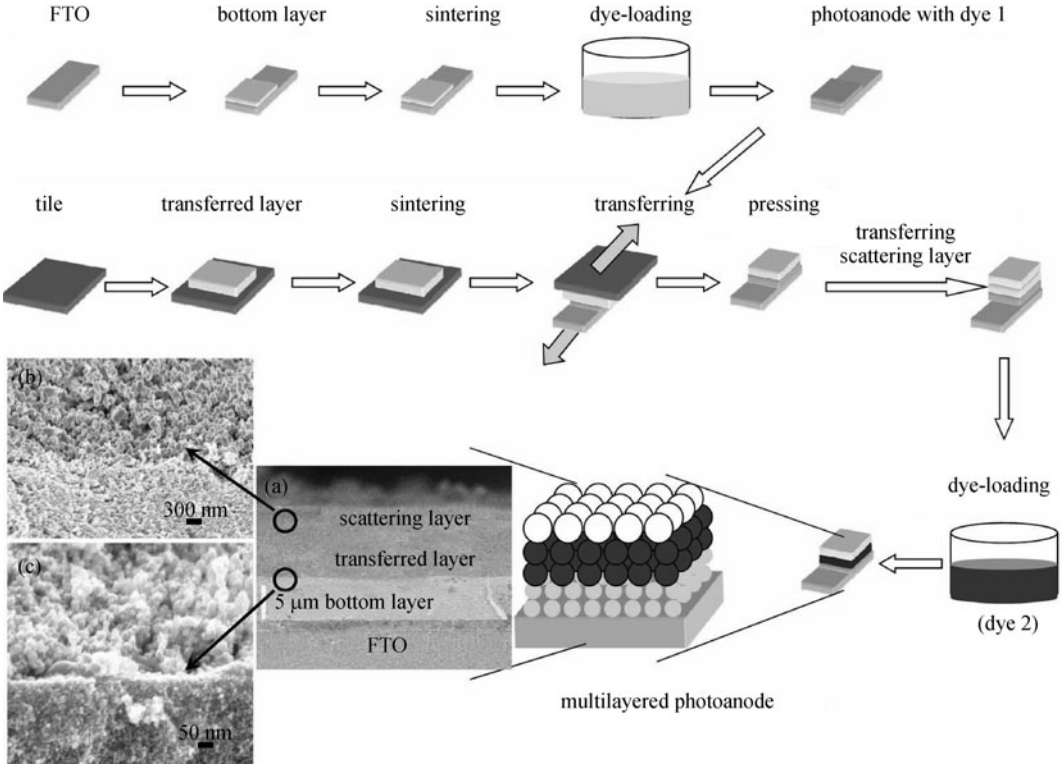

Fig. 4 Schematic diagram of preparation procedure and the scanning electron microscope (SEM) images of multilayered photoanode. (a) cross section; b) interface of the scattering and transferred layers; and c) interface of the transferred and bottom layers (Reprinted from Ref. [15], Copyright (2011), with permission from John Wiley and Sons)

Table 1 Summary of p-type DSSC with their photovoltaic characteristics

electrode	thickness/μm	dye	electrolyte	V_{oc}/mV	J_{sc}/(mA·cm^{-2})	η/%	Ref.
NiO	1	TPPC	0.5 M LiI/0.05 M I_2	98.5	0.079	0.0033	[20]
		erythrosin B		82.8	0.232	0.0076	
NiO	4.2	dye 3	iodide/triiodide	208±3	6.36±0.15	0.46±0.02	[21]
	6.0			185±3	7.0±0.30	0.43±0.01	
NiO	1	erythrosin B	0.5 M LiI/0.05 M I_2	83	0.269	0.0071	[22]
NiO	none	NK-2684	I^-/I_3^- electrolyte	93	2.0	0.027	[23]
NiO	1.6	erythrosin J	0.5 M LiI/0.05 M I_2	122±3	0. 36±0.12	0.011±0.001	[24]
		eosin B	0.5 M LiI/0.05 M I_2	77±8	0. 14±0.02	0.0032±0.0001	
NiO	35	C343	0.6 M LiI/0.3 M I_2	113	1.61	0.057	[25]
NiO	1.6	C343	0.5 M LiI/0.05 M I_2	98±8	0. 55±0.14	0.016±0.004	[24]
			0.5 M LiI/0.5 M I_2	65±10	1.15±0.35	0. 025±0.006	
			0.5 M LiI/2 M I_2	37±2.4	2.13±0.2	0.024±0.003	
NiO	0.6	C343	0.5 M LiI/0.1 M I_2	70	0.78	0.017	[26]
		P1		110	1.52	0.052	
NiO	2.4	C343	0.7 M LiI/0.05 M I_2	101	0.86	0.031	[27]
NiO	3.5	C343	I^-/I_3^- electrolyte	117	0.88	0.036	[28]
		PMI-NDI dyad		370	1.3	0.16	
NiO	1.7	fast green FCF	0.7 M LiI/0.05 M I_2	93	1.44	0.043	[27]
	2.2	NKX-2311		100	0.66	0.022	
	2.1	NK-3628		77	0.43	0.011	
	1.8	NK-2612		73	0.45	0.013	
NiO	1–1.4	P1	1 M LiI/0.1 M I_2	110	2.51	0.08	[29]
		P4		100	2.48	0.09	
NiO	5	PINDI	$Co^{II/III}$ couple	350	1.7	0.2	[30]
		PI		80	0.26	0.006	
		C343		190	0.25	0.015	
NiO	1.1–1.2	P1	1 M LiI/0.1 M I_2	106	3.01	0.12	[31]
		P1		84	5.48	0.15	
		C343		71	1.89	0.05	
NiO	1.2	P2	1 M LiI/0.1 M I_2	63	3.37	0.07	[32]
		P3		55	1.36	0.03	
		P7		80	3.37	0.09	

(*Continued*)

electrode	thickness/μm	dye	electrolyte	V_{oc}/mV	J_{sc}/(mA·cm^{-2})	η/%	Ref.
NiO	3.3	dye 1	iodide/triiodide	153	2.06	0.09	[33]
		dye 2		176	3.40	0.19	
		dye 3		218	5.35	0.41	
NiO	1.55	dye 3	iodide/triiodide	227	3.87	0.30	[34]
	X			350	0.04	0.01	
	X + 0.1			305	1.32	0.14	
NiO	0.9	dye 3	iodide/triiodide	301	2.6	0.33	[35]
	1.7			292	3.3	0.40	
NiO	0.6	O2	1.0 M LiI/0.1 M I_2	94	1.43	0.05	[36]
		O6		97	1.04	0.037	
		O7		90	1.74	0.06	
		O8		63	0.44	0.009	
NiO	0.6	O11	1.0 M LiI/0.1 M I_2	79	1.16	0.033	[37]
		O12		82	1.84	0.051	
NiO	ruthenium sensitizers 1		1.0 M LiI/0.1 M I_2	85	0.63	0.019	[38]
	ruthenium sensitizers 2			95	0.78	0.025	
	ruthenium sensitizers 3			75	0.25	0.0065	
	ruthenium sensitizers 4			85	0.65	0.018	
	C343			95	0.87	0.03	
NiO	2	PMINDI	Co(ttb-tpy)$_2$(ClO$_4$)$_{2/3}$PC	240	1.61	0.13	[39]
			Co(dtb-bpy)$_3$(ClO$_4$)$_{2/3}$PC	340	2.00	0.24	
			Co(dMeO-bpy)$_3$(PF$_6$)$_{2/3}$ MeCN	200	2.42	0.17	
			Co(dtb-bpy)$_3$(PF$_6$)$_{2/3}$MeCN	275	2.65	0.24	
$CuAlO_2$	1.6	Dye 3	iodide/triiodide	333	none	0.041	[40]
$CuGaO_2$	3.03	P1	1.0 M LiI/0.1 M I_2	180	0.384	0.026	[41]
			0.1 MCo^{3+}/0.1 MCo^{2+}	357	0.165	0.018	
$CuGaO_2$	1.5	PMINDI	0.1 M LiI/1 M I_2	187	0.29	0.023	[42]
			Co^{2+}/Co^{3+}	375	0.12	0.0149	

Note: 1 M = 1 mol·L^{-1}

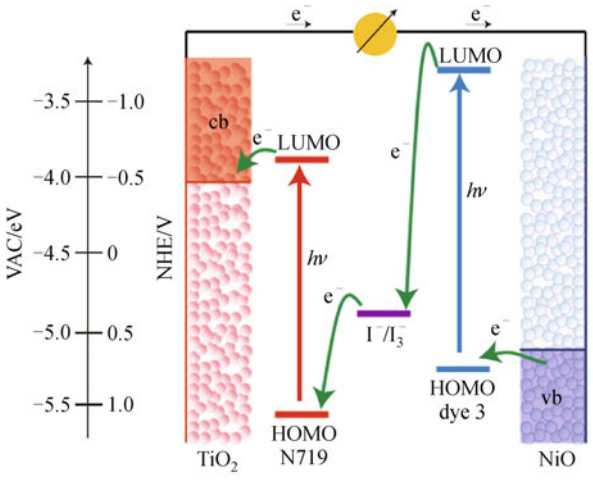

Fig. 5 Schematic show of working principle of n-p tandem structured DSSC (Reprinted from Ref. [33], Copyright (2010), with permission from Macmillan Publishers Ltd: [Nature Materials]) (HOMO: highest occupied molecular orbital, LUMO: lower unoccupied molecular orbital, VAC: vacuum level, NHE: normal hydrogen electrode)

achieve the satisfaction of the photoelectric conversion efficiency [2,4]. For sufficient dye adsorption, 2 μm thick NiO film obviously is not sufficient. But it may be due to that NiO film is not fully optical transparent, too much thicker film will lead to many adsorbed dyes in the shade of NiO. Another possible reason might be ascribed to the limited effective hole diffusion length hindered by the slow diffusion coefficient of NiO. Nevertheless, Fujihara and coworkers reported a p-type DSSC based on C343 dye sensitized NiO film with the thickness of approximately 35 μm, which still yielded a V_{oc} of 113 mV, J_{sc} of 1.61 mA $\cdot cm^{-2}$ and η of 0.057% [25].

In the typical NiO based DSSC, low photocurrent is due to fast charge recombination between the reduced dye and the holes generated in the NiO, and the low light-harvesting efficiency resulting from the limited dye loading on the NiO film. Photoinduced absorption spectroscopy measurements indicate that the hole diffusion coefficient (D) in NiO films is in the range of 10^{-8} to 10^{-7} $cm^2 \cdot s^{-1}$ (4×10^{-8} $cm^2 \cdot s^{-1}$ [27], 1.6×10^{-7} $cm^2 \cdot s^{-1}$ [31], 1.3×10^{-8} $cm^2 \cdot s^{-1}$ [48]), and the hole lifetime depends on light intensity, ranging from 3×10^{-2} to 1×10^{0} s [27]. The value of D was 3 orders of magnitude lower than the typical value of D for electrons in nanocrystalline TiO_2 based DSSC, while the hole lifetime was comparable to the electron lifetime in nanocrystalline TiO_2 based DSSC. To improve the hole transport and slow down the charge recombination in photocathode, several attempts on the semiconductive electrode have been implemented and achieved some exciting results. Based on the studies of n-type DSSC, the semiconductor surface coated with a thin layer of insulated material could restrain the charge recombination process effectively. Mori and coworkers [49] and Majima and coworkers [50] coated the porous NiO electrodes with Al_2O_3 by dipping in an aluminum alkoxide solution. The V_{oc}, J_{sc} and η of the treated DSSCs were all higher than that of non-treated counterparts.

Moreover, several works have studied various microstructures of NiO photocathodes to enhance the performance of the p-type DSSC. Bach and coworkers reported a highly crystalline nanostructured nickel (II) oxide microballs (NiO-μBs) developed for p-type DSSC recently [21]. The recorded J_{sc} for p-type DSSC was obtained accordingly, with the remarkable value of 7.0 mA $\cdot cm^{-2}$. The optimal η of 0.43% was achieved for NiO photocathode with thickness of 6.0 μm. Bach and coworkers later reported a p-type DSSC based on efficient dye 3 sensitized highly crystalline NiO nanoparticles, a remarkably enhanced V_{oc} of 350 mV was obtained, but the J_{sc} of 0.04 mA $\cdot cm^{-2}$ was too low if without a dense blocking layer [34]. With a 100 nm compact underlayer, an improved J_{sc} of 1.32 mA $\cdot cm^{-2}$ and η of 0.14% were obtained. They also reported a NiO nanorod based photocathode with a blocking layer [35] achieved an optimized performance at the thickness of 1.7 μm, with the V_{oc} of 292 mV, J_{sc} of 3.3 mA $\cdot cm^{-2}$ and η of 0.40%; the results are very closed to the record of p-type DSSC (0.46% in efficiency). They demonstrated that the short hole diffusion length (about 2 μm) and the insufficient charge collection (about 0.8) may account for the relatively low fill factors found in the p-type DSSCs. Therefore, to find other p-type semiconductors alternative to NiO with reasonable higher hole diffusion coefficient is another way to improve the performance of p-type DSSC.

Recently promoted delafossite ABO_2 materials, including $CuAlO_2$ [40] and $CuGaO_2$ [41,42], which belong to the important family of transparent conducting oxides, feature excellent optical transparency in the visible range and high electrical conductivity [51,52], have been demonstrated to be a very promising alternative to NiO in p-type DSSC. V_{oc} of the reported cells based on ABO_2 p-type semiconductors have been proved to be 50–150 mV higher than that of the NiO base, associated with their deeper valance band edge positions [40–42]. Cheng and coworkers reported DSSC using the p-type semiconductor $CuAlO_2$, a peak IPCE value of 4.0%, V_{oc} of 333 mV and η of 0.041% were obtained. The V_{oc} for the $CuAlO_2$ based p-type DSSC was substantially higher than that of NiO based p-type DSSC sensitized with PMI-6T-TPA (333 mV compared to 218 mV) [40].

3.2 Sensitizers used in p-type DSSC

In a typical p-type DSSC, the sensitizer after excitation injects a hole into the valence band (VB) of the semiconductor and transfers electrons to the electrolyte upon light absorption, so that the separation of electrons and holes produce the photocurrent and photovoltage in DSSC. Thus, efficient sensitizers should possess the

following features: 1) absorb across a broad range of the solar spectrum (panchromatic dye) in order to harvest the greatest number of photons; 2) photochemically and electrochemically stable to ensure the stability of the cell over a long period of time; 3) suitable HOMO level lies above the valence band edge of the semiconductor and LUMO level below the potential of redox mediator, to allow efficient interfacial charge separation; 4) high light extinction coefficient to harvest more solar light within a thinner photocathode, allowing the holes diffuse a shorter path length to reach the charge collection substrate [5–7]. Various dyes sensitized NiO based solar cells have been reported yet to date, such as erythrosine [20,22], coumarin [24,25,30,53,54], porphyrin [55], fast green FCF [27], a series of NK (2684, 3628, 2612) [27] and NKX (2311, 2586, 2753, 2593) [56], a series of P1 (P1, P2, P3, P4, P7) [26,29,31,32], a series of peryleneimide-based dyes (PI, PI-NDI, PMI, PMI-NDI) [28,30,41,42,57], a series of modified PMI (dye 1, dye 2, dye 3) [33–35], donor-acceptor dyes (O2, O6, O7) [36], cyclometalated Ru(II) complexes (O8, O11 and O12) [37], ruthenium complexes (1–4) [38] and Atto647N [58,59].

In the first "p-type DSSC" reported in 1999, the NiO electrodes were sensitized by tetrakis (4-carboxyphenyl) porphyrin (TPPC) and erythrosin B, the cathodic photocurrent was for first time detected and explained by hole injection from dye molecule to the valence band of NiO [20]. Coumarin 343 (see Fig. 6) dye was first reported in p-type DSSC by Hammarström and coworkers [53]. The photoinduced electron transfer from NiO to coumarin 343 dye was found to have an ultrafast component (200 fs), which was comparable to electron transfer from coumarin 343 dye to TiO_2 [54]. Back electron transfer from NiO to coumarin 343 dye was found to be also remarkably fast, the recombination process happened with a time constant of 20 ps. The fast recombination may be the inherent cause accounting for the poor performance of p-type DSSC [53]. At present, coumarin 343 is commonly used as a sensitizer in p-type DSSC and has become a benchmark reference. It gave J_{sc} values from 0.25 to 2.13 $mA \cdot cm^{-2}$, V_{oc} values from 37 to 190 mV, and η in the range of 0.015%–0.057%, depending on the preparation methods of NiO films and different electrolytes applied (see Table 1). The highest J_{sc} of 2.13 $mA \cdot cm^{-2}$ based on coumarin 343 sensitized NiO photocathode was reported by Bach and coworkers in 2008, the morphology, thickness and the sintering condition of NiO film had been thoroughly optimized [24]. The highest V_{oc} of 190 mV for coumarin 343 sensitized DSSC was reported by Odobel and coworkers in 2009 by using a cobalt-based electrolyte [30].

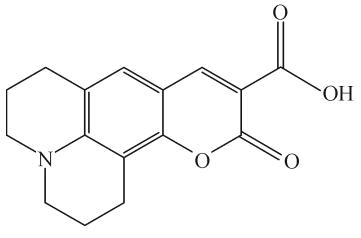

Fig. 6 Molecular structure of coumarin 343 (Reprinted with permission from Ref. [54], Copyright (1996), American Chemical Society)

Several works have studied the coumarin derived dyes, reported by Mori et al. [27] and Sánchez-de-Armas et al. [56], such as fast green FCF, NKX-2311, NK-2684, NK-3628, NK-2612, NKX-2311, NKX-2586, NKX-2753 and NKX-2593 (see Fig. 7). The absorption threshold and the HOMO energy with respect to the valance band edge of p-type semiconductor are key parameters in order to establish some criteria that allow evaluating the efficiency of coumarin derivatives as sensitizers in DSSC [56].

In 2008, Sun and coworkers first reported a series of donor-π-acceptor dyes (see Fig. 8, P1, P2, P3, P4 and P7) for sensitization on NiO photocathode [26,29,31,32], the maximum 63% and minimum 6% of IPCE were achieved based on these dyes. The femtosecond transient absorption spectroscopy shows a fast injection rate of more than 250 fs^{-1} for these dyes, and the injection efficiency reaches 90% [32]. By optimizing the NiO electrode film, a p-type DSSC with V_{oc} of 84 mV, J_{sc} of 5.48 $mA \cdot cm^{-2}$ and η of 0.15% was obtained [31]. It is the first time that the donor-π-acceptor concept was applied to design and investigate the dye matching p-type semiconductor, which could be regarded as a milestone on the development of efficient p-type dyes.

In 2009, Hagfeldt and coworkers reported peryleneimide (PI) and peryleneimide-naphthalenediimide dyad (PINDI) dyes sensitization on NiO photocathode (see Fig. 9). The latter dye exhibits a substantial retardation of the charge recombination between the hole and the reduced PINDI dye in comparison to the PI dye, approximately 10^5 times slower [30]. The absorbed-photon to current conversion efficiency (APCE) was three times higher with the PINDI dye than that with the PI dye (45% vs 15%) [57]. Odobel and coworkers reported a p-type DSSC based on the improved PINDI dye as sensitizer and the $cobalt^{II/III}$ couple as redox mediator, V_{oc} of 370 mV, J_{sc} of 1.3 $mA \cdot cm^{-2}$ and η of 0.16% were achieved, and the V_{oc} of 370 mV is the highest record of NiO based p-type DSSCs until now [28].

As the linker group between the donor and the acceptor plays an key role in terms of optical absorption and charge transfer properties in a donor-acceptor dye, in 2010 Bach and coworkers reported three donor-acceptor type dyes, called dyes 1–3, Fig. 10, comprising a perylenemonoimid (PMI) as the acceptor and an oligothiophene coupled to triphenylamine as the donor [33]. The dye molecules (dyes 1–3) tend to slow recombination between the photo-reduced sensitizer and the NiO, and also help to shield the NiO surface from the triiodide/iodide redox mediator, as increased hydrophobicity of dyes with increasing length of

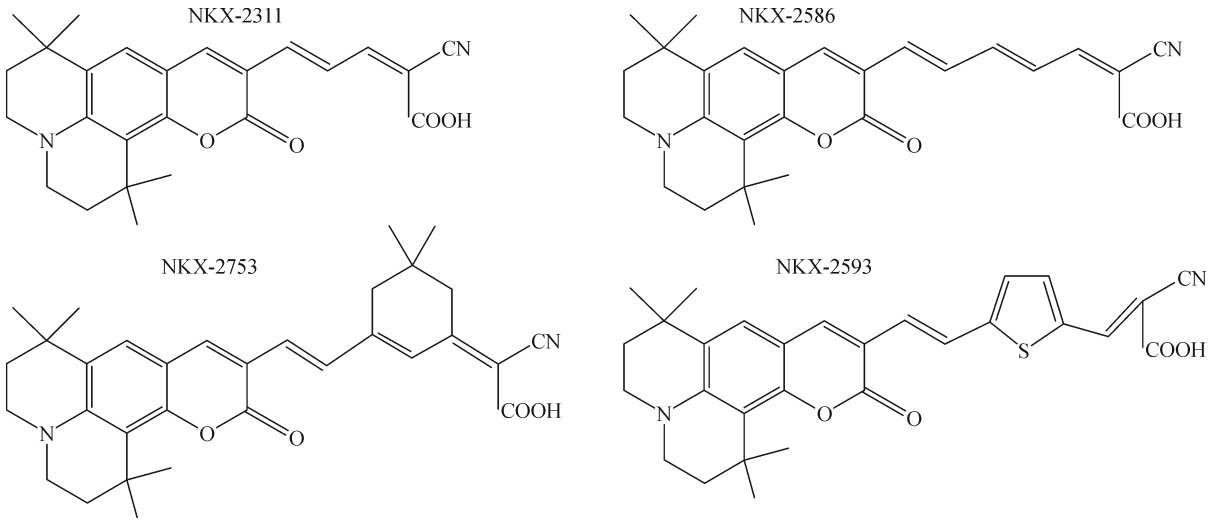

Fig. 7 Structures of dyes (NKX-2311, NKX-2586, NKX-2753 and NKX-2593) [56]

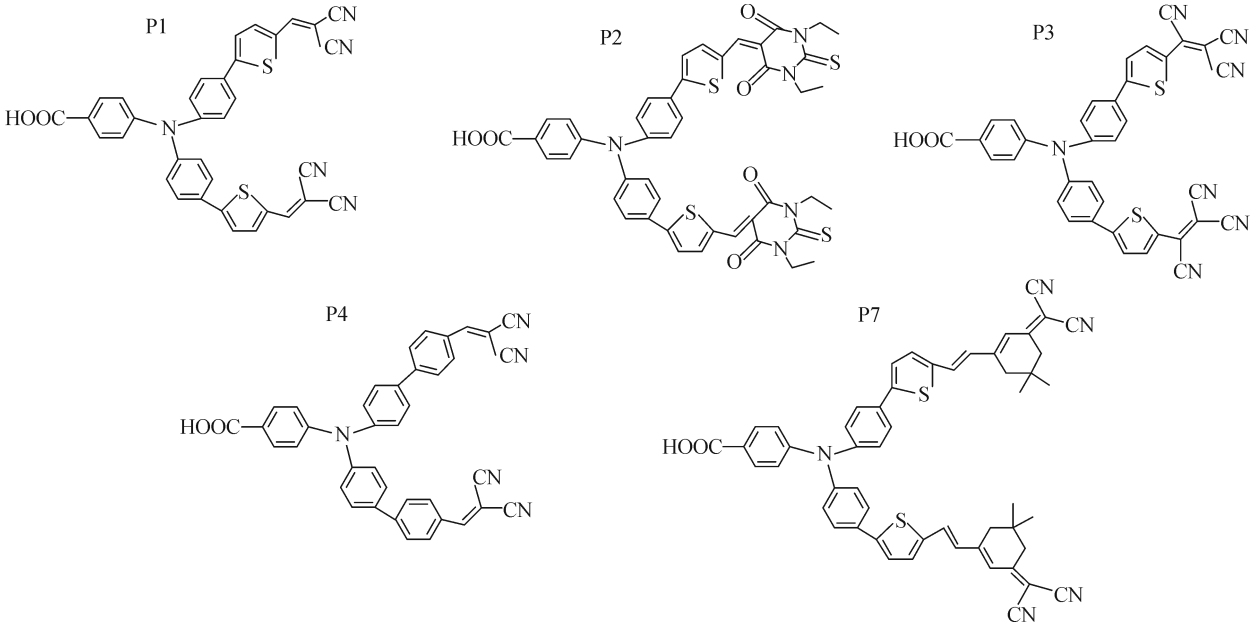

Fig. 8 Molecular structures of P1, P2, P3, P4 and P7 (Reprinted with permission from Ref. [32], Copyright (2010), American Chemical Society)

the oligothiophene linker [33]. A high η of 0.41% for p-type DSSC based on dye 3 sensitized NiO nanoparticle film was obtained in their first report on this dye. Latter, by improving the photocathode, a record IPCE of 74% was reached; the record η for p-type DSSC with V_{oc} of 208 mV, J_{sc} of 6.36 mA·cm^{-2} and η of 0.46% were achieved based on dye 3.

Wu and coworkers reported the O-series dyes with the Ru(II) complex structures (Fig. 11) [36], since the dye structures were popular in the conventional n-type DSSCs, due to their advantages in the stability, structural flexibility and synthetic accessibility. Kinds of ruthenium complexes have been examined as sensitizers in NiO based p-type DSSCs recently [37]. V_{oc} of 82 mV, J_{sc} of 1.84 mA·cm^{-2} and η of 0.051% were obtained based on O12 sensitized NiO nanorod film. The performance of p-type DSSCs based on O7/O12 sensitized NiO photocathode were comparable to that of the best record achieved by coumarin 343 sensitized NiO, reflecting that these stable dyes are promising alternative to coumarin 343 in p-type DSSC. Besides the above works, Jacquemin and coworkers reported four ruthenium trisbipyridine complexes (1–4) in NiO based p-type DSSC in 2011, and they claimed that carboxylic acid displayed the highest affinity for NiO surface, which significantly bind to NiO surface [38]. Yeow and coworkers reported the hole transfer dynamics of Atto647N [58] dye sensitized on thin films made of NiO nanoparticles recently [59].

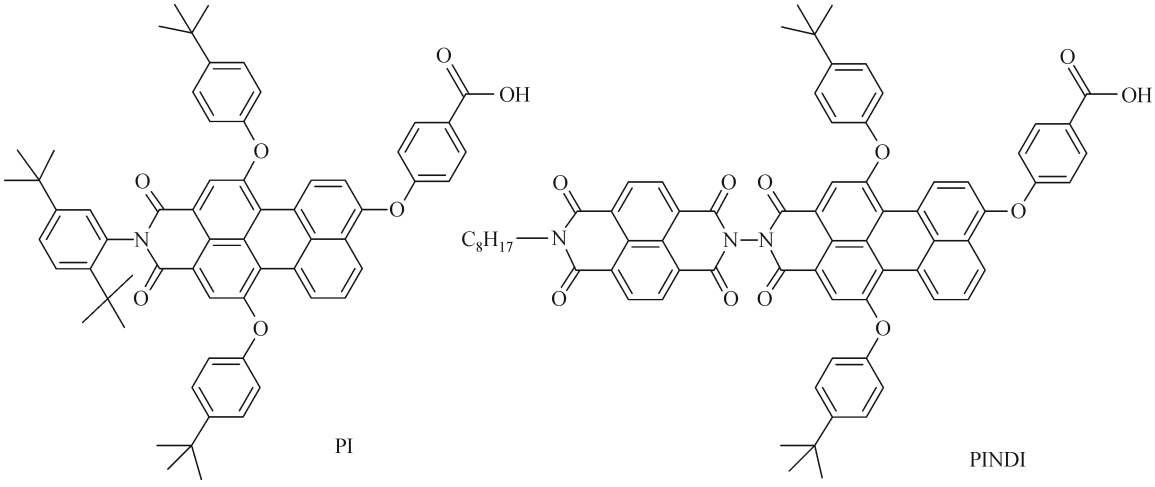

Fig. 9 Molecular structures of PI and PINDI (Reprinted with permission from Ref. [30], Copyright (2009), John Wiley and Sons)

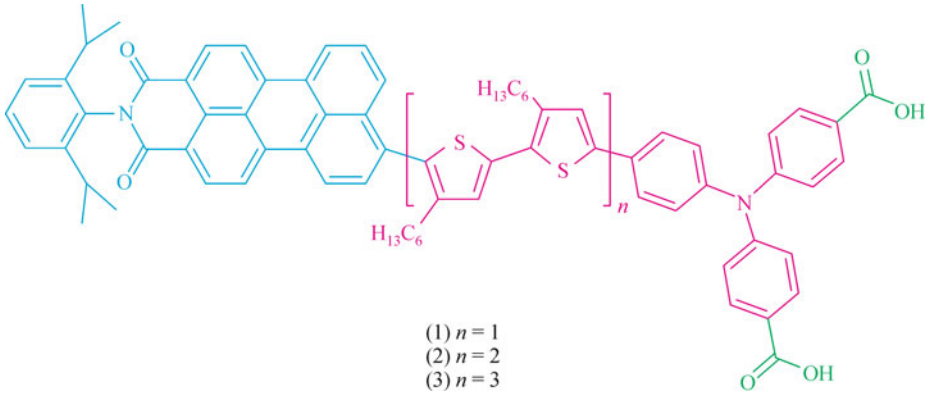

Fig. 10 Chemical structure of donor-acceptor dyes 1–3(Reprinted from Ref. [33], Copyright (2010), with permission from Macmillan Publishers Ltd: [Nature Materials])

It can be expected that, the design on molecular structure of p-type dye is essential for the further improvement on the performance of p-type DSSC. The most promising dyes should first consider the donor-π-acceptor design similar to the P1 dye and dye 3. And, due to the fact that neither the P1 dye nor the dye 3 dye has much narrower light absorption range than that of the efficient dyes applied in n-type DSSCs, to expand the light absorption range of p-type dyes is also in urgent need.

3.3 Electrolytes used in p-type DSSC

The role of the redox mediator in p-type DSSC is to regenerate the reduced sensitizers after the hole injections to the p-type semiconductor and to transport the electrons to the counter electrode. To fulfill the function, the redox mediator should meet the following requirements: 1) The redox potential must be more negative than that of the valance band edge of semiconductor, to ensure a decent V_{oc} of p-type DSSC dependent upon their difference; 2) the redox mediator almost does not absorb significantly in the visible region (400–800 nm), so that the dye can utilize the sunlight more sufficiently, 3) the electron self-exchange rate and diffusion coefficient of redox couple must be high, in order to ensure a quick transport of the charges to the counter electrode [5–7].

Until now, the iodide/triiodide electrolyte is commonly used as redox mediator in p-type DSSC, but its drawbacks are also evident. The biggest issue should be assigned to too small potential offset between the valence band of NiO and redox potential of iodide/triiodide electrolyte, leading to too small V_{oc} of corresponding p-type DSSC. The second problem might be the visible light absorption, especially in case of a relatively high concentration of iodine [5–7]. Bach and coworkers reported the coumarin 343 sensitized NiO based DSSCs with the electrolytes containing I_2 concentrations varying from 0.05, 0.5 to 2 M (0.5 M LiI was used throughout). V_{oc} of the cell was found to decrease with increasing iodine concentrations, while J_{sc} increased dramatically. When a 2 M iodine based electrolyte was used, J_{sc} of 2.13 mA·cm^{-2} was obtained, which was the highest value reported so far for p-type DSSC

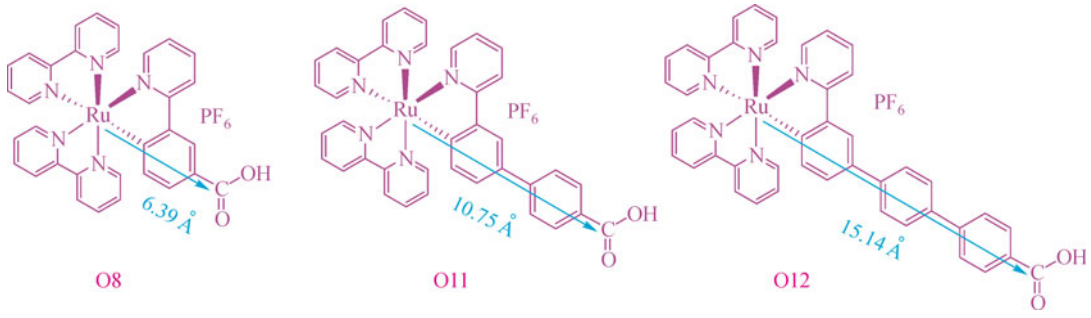

Fig. 11 Structures of series dye with O8, O11 and O12 (Reprinted with permission from Ref. [37], Copyright (2012), American Chemical Society)

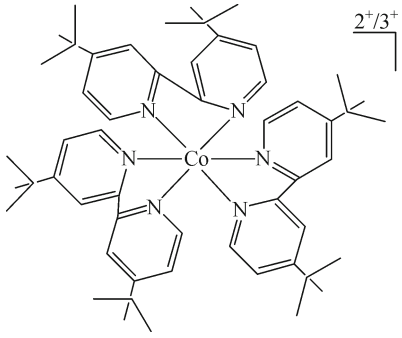

Fig. 12 Molecular structure of $Co^{II/III}$ tris(4,4′-di-ter-butyl-2,2′-dipyridy1) (Reprinted with permission from Ref. [30], Copyright (2009), John Wiley and Sons)

based on coumarin 343 dye [24]. Hammarström and coworkers also checked the influence of iodine concentration in the electrolyte on charge separation and the charge recombination kinetics in p-type DSSC [60].

Compared with iodide/triodide electrolyte, the cobalt-based electrolyte is optically dilute and the Nernst potential of the $Co^{II/III}$ couple is more negative than that of iodide/triodide. In 2009, Odobel and coworkers first reported a complex of $Co^{II/III}$ tris (4,4′-di-ter-butyl-2,2′-dipyridy1) perchlorate (see Fig. 12) used as a new redox mediator in NiO based p-type DSSC [30]. They demonstrated a V_{oc} of 190 mV by using cobalt-based redox mediator, which was almost twice higher than the classical iodide/triodide electrolyte (100 mV). For the newly reported $CuGaO_2$ based p-type DSSCs, $Co^{II/III}$ couple based electrolyte also gave rise to almost twice V_{oc} of the cell than that achieved by iodide/triodide electrolyte (357 mV vs 180 mV, 375 mV vs 187 mV) [41,42]. Furthermore, Boschloo and coworkers reported a series of polypyridyl cobalt complexes with different substituents, which were applied as redox mediators in p-type DSSC based on PMI-NDI dye sensitized NiO recently [39]. Their work reflected that the photocurrent and photovoltage of the devices were dependant on the steric bulk of the redox species, and the charge recombination between holes in NiO and the electrolyte redox couple was restrained by the bulky substituents. Based on two kinds of $Co^{III/II}$ electrolytes (Co(dtb-bpy)$_3$(ClO$_4$)$_{2/3}$PC and Co(dtb-bpy)$_3$(PF$_6$)$_{2/3}$MeCN),

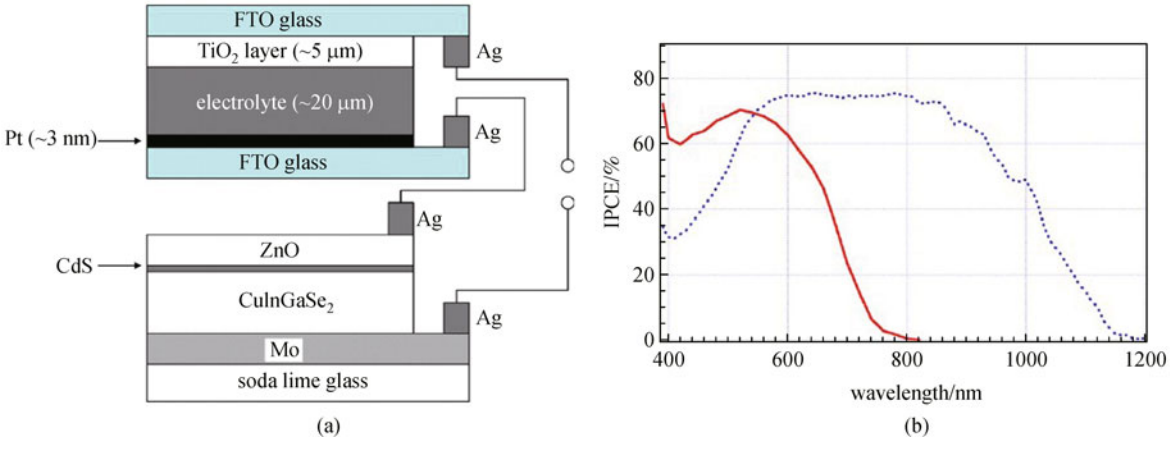

Fig. 13 (a) Schematic representation of DSSC/CIGS structure, DSSC and CIGS are series connected (Reprinted from Ref. [63], Copyright (2010), with permission from Elsevier); (b) spectral response curves of photocurrent for DSSC top cell (bold line) and a red and near IR sensitive bottom cell (dotted line) (Reprinted with permission from Ref. [62], Copyright [2006], American Institute of Physics)

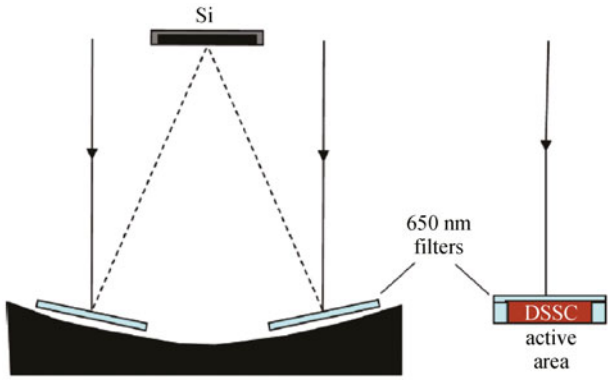

Fig. 14 Illustration on structure and working principle of tandem positioned DSSC and Si solar cell (Reprinted with permission from Ref. [66], Copyright (2011), American Chemical Society)

PMI-NDI dye sensitized NiO based DSSCs achieved V_{oc} of 340 mV, J_{sc} of 2.0 mA·cm^{-2}, η of 0.24%, and V_{oc} of 275 mV, J_{sc} of 2.65 mA·cm^{-2}, η of 0.24%, respectively.

3.4 Progress on tandem devices

The n-p tandem structured DSSC, in physical, is another kind of series-connected tandem structured DSSC. Its V_{oc} depends on the potential difference between the valence band edge of the p-type semiconductor and the conduction band edge of the n-type semiconductor used in both side electrodes. A substantial increase of V_{oc} is certainly a pertinent strategy to enhance η of DSSC. But J_{sc} of n-p tandem structured DSSC is too low in the current state, which is mainly limited by the p-type subcell.

Lindquist and coworkers first reported an erythrosin B sensitized NiO photocathode (1 μm thick) in combination with a N719 sensitized TiO_2 photoanode (4.4 μm thick), which produced a tandem device with V_{oc} of 732 mV, which is the sum of the subcells (650 mV for TiO_2 based DSSC and 83 mV for NiO based DSSC). The J_{sc} of this n-p tandem structured DSSC was 2.26 mA·cm^{-2}, which was much lower than that of the n-type DSSC (7.16 mA·cm^{-2}) but higher than that of the p type one (0.269 mA·cm^{-2}). Finally the η was as low as 0.39% [22]. Later, Suzuki and coworkers have studied the irradiation direction effecting on the n-p tandem structured DSSC; they demonstrated that the irradiation direction did not make a significant difference on the tandem device's performance [23]. To match the anodic and cathodic photocurrent in n-p tandem structured DSSC, Odobel and coworkers designed specific film thicknesses for photoanode and photocathode respectively (5 μm TiO_2 film and 1.5 μm NiO film) to give nearly equal J_{sc} of the n-type subcell (1.7 mA·cm^{-2}) and the p-type subcell (0.97 mA·cm^{-2}). They finally obtained a η of 0.55% for the tandem structured DSSC [30]. Furthermore, the optimal thicknesses of the photoanode and the photocathode are also related to the incident direction of sunlight. Bach and coworkers reported an n-p tandem structured DSSC consisting of a N719 sensitized TiO_2 photoanode and a dye 3 sensitized NiO photocathode [33]. When the tandem device was illuminated through the n-side, film thicknesses should be optimized at 0.8 μm for TiO_2 film and 3.3 μm for NiO film, the V_{oc} of this n-p tandem structured DSSC was 1079 mV, the J_{sc} was 2.4 mA·cm^{-2} and the η was 1.91%. However, as demonstrated in the same work, when the n-p tandem structured DSSC was illuminated through the p-side, the optimal thicknesses should be 12 μm for TiO_2 film and 1.55 μm for NiO film, the V_{oc} of the tandem device was 958 mV, J_{sc} of 4.07 mA·cm^{-2} and η was reached 2.42%.

In short, in comparison to both of the single n-type DSSC and p-type DSSC, few studies have focused on n-p tandem structured DSSC. Further intensive researches are needed. The performance record for n-p tandem structured DSSC was still only 2.42%, but the fast progress achieved in recent years on the p-type DSSC field make the future of this design very promising. The bottleneck of n-p tandem structured DSSC rests with how to improve the performance of p-type single cell. New p-type semiconductors with deeper valance band edges, new dyes with wide light absorption, new redox mediator matched both the n-type photocathode and p-type photoanode, all need to be widely explored. Intensive basic researches for understanding the sensitization effect of dyes on p-type semiconductors, the hole injection and charge separation processes at the p-type semiconductor/dye/electrolyte interfaces are required. It could be expected that, for the single p-type DSSC, if J_{sc} could be increased from currently about 6–7 mA·cm^{-2} to above 12 mA·cm^{-2}, V_{oc} could be improved from currently about 0.2–0.3 V to be about 0.5–0.6 V, the n-p tandem device with J_{sc} of 12 mA·cm^{-2}, V_{oc} of 1.3–1.4 V, and an overall solar conversion efficiency of 12.5%–13.5% could be obtained with an assumed fill factor of 0.8.

4 DSSC tandems with other solar conversion devices

Owing to the specific optical transparent and color tunable features of DSSC, various solar conversion devices [61–71], such as other type solar cells, thermoelectric device, photoelectrochemical (PEC) cell for water splitting, etc., have been demonstrated to work together with DSSC in recent years. In different combinations, the function of DSSC is set differently, but basic principles are common for kinds of hybrid devices. That is to broaden the solar spectrum utilization range with two or more light absorbers from different single devices.

4.1 DSSC tandem with other type solar cells

Solar cells tandem with DSSC should consider the optical matching between different light absorbers. Because the

absorption range of DSSC and copper indium gallium selenide (CIGS) solar cell (Fig. 13(b)) closely match the ideal optical gap requirements for a double-junction tandem device [61], DSSC tandem with CIGS solar cell were frequently reported [62–65]. The typical configuration of the tandem structured cell is shown in Fig. 13(a). Grätzel and coworkers first reported a tandem structured solar cell comprising a DSSC as the top cell capturing high-energy photons and a CIGS thin-film solar cell as the bottom cell for harvesting lower-energy photons in 2006; the conversion efficiency of 15.09% was achieved, which was higher than that of the DSSC and CIGS single cells [62]. Lin and coworkers reported a similar tandem design composed of DSSC and CIGS solar cell in 2010. It was found that the transmittance and performance of the DSSC top cell were the essential factors which determined the tandem effect [63]. Similar work was reported in 2011 by Park and coworkers, their series-connected DSSC and CIGS solar cell achieved V_{oc} of 1435 mV, J_{sc} of 14.1 mA·cm^{-2} and η of 12.35%. The IPCE response of the DSSC/CIGS tandem structured solar cell was found to be sensitive to the bias light intensiy [64]. Similar to CIGS (band gap E_g = 1.1 eV), GaAs is another ideal light absorber with band gap of 1.4 eV. In 2011, Ito and coworkers reported a tandem structured solar cell with DSSC as the top cell and a GaAs/$Al_xGa_{(1-x)}As$ graded solar cell (GGC) as the bottom cell. The V_{oc} of GGC and DSSC single cells were 1.11 and 0.76 V, resulting in a remarkable V_{oc} of 1.85 V for the tandem cell, of which the efficiency was 7.63% [65].

To utilize both direct and diffusely scattered visible light while directing the low-scattering near-IR light onto the more efficient Si cell, Greg and coworkers in 2011 [66] proposed a tandem structured solar cell by using DSSC as the 650 nm short-band pass filter positioned on top of the concentrator (see Fig. 14), photons with wavelength longer than 650 nm could pass through the DSSC modules freely and be reflected to the Si solar cell. The proof-of-concept results in the paper suggest that system level efficiencies approaching 20% should be achievable, on the basis of single DSSC with an efficiency of 9.1% and Si solar cell with an efficiency of 18.1%.

In other ways, Jürgen and coworkers first reported a solid-state DSSC combined with a vacuum-deposited bulk hetero-junction (BHJ) solar cell made of zinc phthalocyanine and fullerene in 2009 [67]. The solar cell structure is illustrated in Fig. 15. Since zinc phthalocyanine could harvest the near infrared light, the tandem structured solar cell was demonstrated to have near infrared IPCE response. The reported performance was 1360 mV in V_{oc} and 6.0% in efficiency for the tandem cell, which were remarkably higher than that of the single cells.

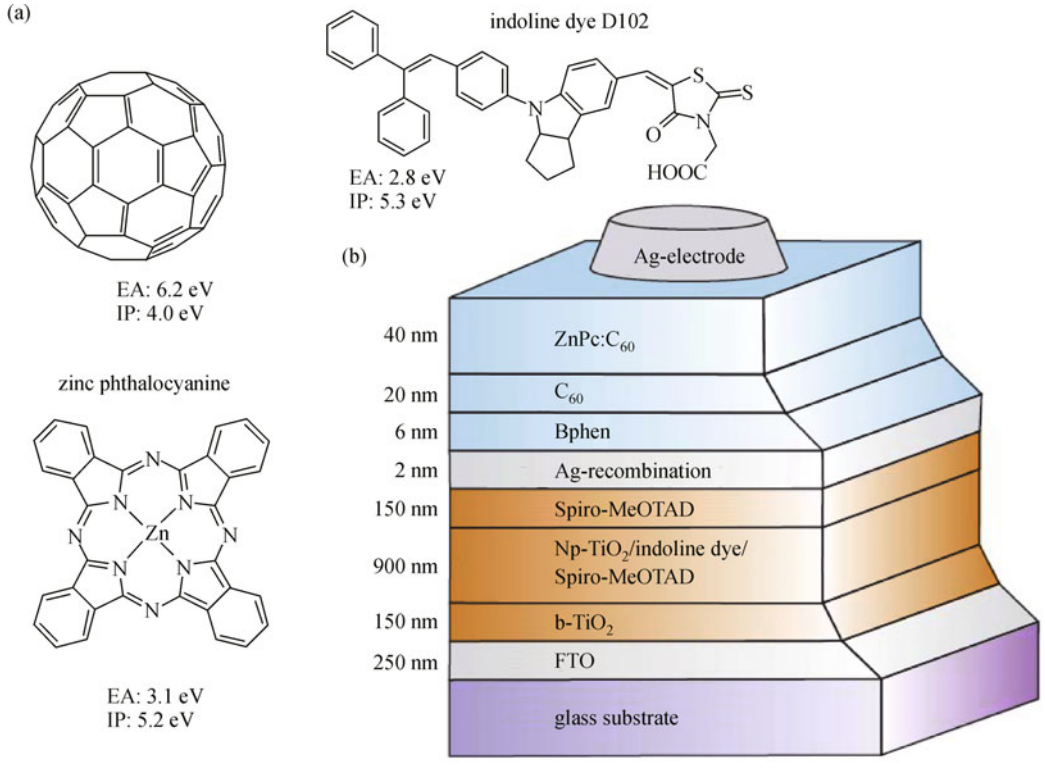

Fig. 15 Illustration on structure of hybrid tandem solar cell based on solid-state DSSC and vacuum deposited bulk heterojunction solar cell (Reprinted from Ref. [67], Copyright (2009), with permission from Elsevier)

4.2 DSSC tandem with thermoelectric cell

Heat in the solar cell was produced from IR irradiation, charge recombination and illumination energy over the sensitizer energy gap. Conversion of the "waste heat" to useful electricity could improve the overall efficiency of solar cells. Thermoelectric cell can transform a temperature gradient into electricity. It is suggested that in DSSC up to 85% of solar energy was absorbed and more than 60% of which converts to heat instead of electrical energy. Therefore, it is very promising to design a tandem structure comprising DSSC and thermoelectric cell.

In 2010, Meng and coworkers demonstrated the first model of DSSC tandem with thermoelectric cell. The hybrid device comprises a DSSC as the top cell and a thermoelectric cell as the bottom cell [68], as illustrated in Fig. 16. It was reported that the overall conversion efficiency could be improved by optimal designing DSSC module in order to match the output current of the selected thermoelectric cell. Comparing with the individual DSSC, an efficiency increase of 10% has been obtained from the hybrid tandem cell. Wang and coworkers reported a similar hybrid device comprising a DSSC as the top cell and a solar selective absorber coated thermoelectric generator as the bottom cell in 2011 [69]. They got a remarkable V_{oc} of 1210 mV, J_{sc} of 20.3 mA·cm^{-2} and η of 13.8%. The breakthrough should be ascribed to employing Bi_2Te_3 as the thermoelectric material, which is superior to others in converting heat to electricity around the room temperature.

4.3 DSSC tandem with PEC cell for water splitting

WO_3, Fe_2O_3 have reasonable band gap and high stability in aqueous electrolyte, which were generally used as photoanode materials in PEC cells for water splitting [70,71]. However, their conduction band edge energies are too low to generate hydrogen; an external bias is required to help for water splitting. Besides, since band gaps of WO_3 and Fe_2O_3 are only 2.6 and 2.0 eV, a considerable portion of solar irradiation will be wasted. Therefore, design a tandem structure consisting of DSSC and PEC cell is reasonable for efficient water splitting by utilization of more solar energy.

Compared with the solar-to-hydrogen efficiency 1.16% with the standard back DSSC case, depicted as Fig. 17(a), Kevin and coworkers reported a trilevel hematite/DSSC/DSSC architecture (hematite/SQ1 dye/N749 dye, Fig. 17(b)) produced the highest operating current density and thus the highest expected solar-to-hydrogen efficiency 1.36% in 2010, and the solar-to-hydrogen efficiency for the front DSSC case was 0.76%, depicted as Fig. 17(c) [70]. To realize an unassisted water splitting system, Park and coworkers reported a WO_3/Pt bipolar electrode connected with a DSSC in 2011 [71]. The onset potential of the tandem photoanode was negatively shifted by about 0.6 V, which corresponded to the V_{oc} of DSSC used in the tandem device. Unassisted (no external potential bias) water splitting from the tandem cell was demonstrated and the maximum current density was exhibited at around + 0.4 V (vs Pt).

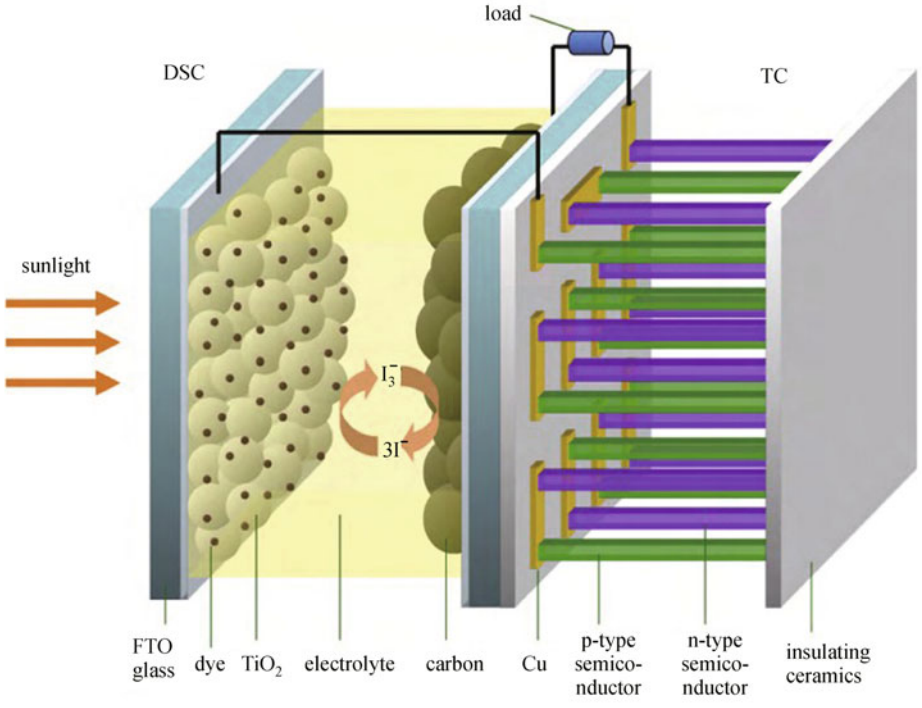

Fig. 16 Two-wire hybrid tandem cell (HTC2) was made by connecting DSSC and TC (thermoelectric cell) (Reprinted from Ref. [68], Copyright (2010), with permission from Elsevier)

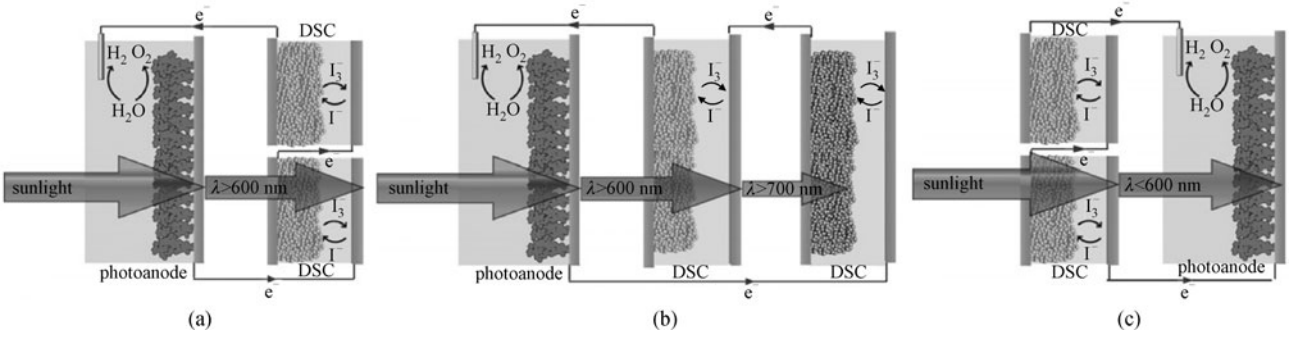

Fig. 17 Layout of three architectures for tandem cell using hematite photoanode and two DSSCs in series. (a) "Back DSSC" configuration; (b) "Trilevel" configuration; (c) "Front DSSC" configuration [70]

5 Conclusions

In short, we have reviewed the recent progresses on kinds of tandem designs associated with DSSC. It has no doubt that the concepts contained in those tandem structured DSSCs provide inspirational information for further development on DSSC technology. The n-n tandem structured DSSCs are more close to efficiency record breaking of the single DSSC, up to the innovation of an efficient near infrared dye which could broaden the strong IPCE response to 1000–1100 nm without significant loss in V_{oc}. The n-p tandem structured DSSCs seem to lag much behind, with the record efficiency of only about 2%, but the progress in recent years became accelerated. It can be expected that only minor extra processing and material costs are needed to fabricate p-n tandem structured DSSCs than the single n-type DSSC, make this technology an economically viable option for the future. Its further improvement relies on the development of transparent nanocrystalline p-type semiconductors with deeper valance band edges, new dyes which could harvest more solar light and work efficiently in combination with the p-type semiconductors, new redox mediators adapt for both n-type DSSC and p-type DSSC. Both of the n-n and n-p tandem designs of DSSC aim to improve the solar cell performance approaching to the applicable threshold easier accepted by the market. Actually, DSSC tandem with other solar conversion devices, which could effectively broaden the application diversity of DSSC technology, would also enhance the possibility for the industrial application of DSSC. To further explore new materials and to deeply understand their working mechanisms in the subcells or the single devices and their combinations would provide the basis for further breakthroughs to attain high performance tandem structured DSSCs. Just like the steady progresses which have been made in the fields of the organic tandem cell and the highly efficient multifunction thin film solar cells used in the aerospace, tandem structured DSSCs we believe would have a bright future.

Acknowledgements The authors would like to express sincere thanks for the financial supports by the National Natural Science Foundation of China (Grant No. 21103058), the National Basic Research Program of China (No. 2011CBA00703), Natural Science Foundation of Hubei Province (No. 2011CDB033) and Basic Scientific Research Funds for Central Colleges (No. 2010QN024). We also thank Analytical and Testing Center of Huazhong University Science and Technology for the sample measurements.

References

1. O'Regan B, Grätzel M. A low-cost, high-efficiency solar cell based on dye sensitized colloidal titanium dioxide films. Nature, 1991, 353 (6346): 737–740
2. Grätzel M. Dye-sensitized solar cells. Journal of Photochemistry and Photobiology C, Photochemistry Reviews, 2003, 4(2): 145–153
3. Thomas W H, Rebecca A J, Alex B F M, Hal Van R, Joseph T H. Advancing beyond current generation dye-sensitized solar cells. Energy & Environmental Science, 2008, 1(1): 66–78
4. Hagfeldt A, Boschloo G, Sun L, Kloo L, Pettersson H. Dye-sensitized solar cells. Chemical Reviews, 2010, 110(11): 6595–6663
5. Odobel F, Le Pleux L, Pellegrin Y, Blart E. New photovoltaic devices based on the sensitization of p-type semiconductors: challenges and opportunities. Accounts of Chemical Research, 2010, 43(8): 1063–1071
6. Shi J F, Xu G, Miao L, Xu X. p-type and pn-type dye-sensitized solar cells. Acta Physico-Chimica Sinica, 2011, 27(6): 1287–1299 (in Chinese)
7. Odobel F, Pellegrin Y, Gibson E A, Hagfeldt A, Smeigh A L, Hammarström L. Recent advances and future directions to optimize the performance of p-type dye-sensitized solar cells. Coordination Chemistry Reviews, 2012, 256(21–22): 2413–2423
8. Yella A, Lee H W, Tsao H N, Yi C, Chandiran A K, Nazeeruddin M K, Diau E W G, Yeh C Y, Zakeeruddin S M, Grätzel M. Porphyrin-sensitized solar cells with cobalt (II/III)-based redox electrolyte exceed 12 percent efficiency. Science, 2011, 334(6056): 629–634
9. Wataru K, Ayumi S, Takayuki K, Yuji W, Shozo Y. Dye-sensitized solar cells: improvement of spectral response by tandem structure. Journal of Photochemistry and Photobiology A, Chemistry, 2004, 164(1–3): 33–39
10. Dürr M, Bamedi A, Yasuda A, Nelles G. Tandem dye-sensitized solar cell for improved power conversion efficiencies. Applied Physics Letters, 2004, 84(17): 3397–3399

11. Takeshi Y, Yuki U, Shinya A, Hironori A. Series-connected tandem dye-sensitized solar cell for improving efficiency to more than 10%. Solar Energy Materials and Solar Cells, 2009, 93(6–7): 733–736
12. Fan S Q, Fang B Z, Choi H B, Paik S, Kim C, Jeong B S, Kim J J, Ko J. Efficiency improvement of dye-sensitized tandem solar cell by increasing the photovoltage of the back sub-cell. Electrochimica Acta, 2010, 55(15): 4642–4646
13. Masatoshi Y, Nobuko O K, Mitsuhiko K, Kazuhiro S, Hideki S. Optimization of tandem-structured dye-sensitized solar cell. Solar Energy Materials and Solar Cells, 2010, 94(2): 297–302
14. Lee K, Park S W, Ko M J, Kim K, Park N G. Selective positioning of organic dyes in a mesoporous inorganic oxide film. Nature Materials, 2009, 8(8): 665–671
15. Miao Q, Wu L, Cui J, Huang M, Ma T. A new type of dye-sensitized solar cell with a multilayered photoanode prepared by a film-transfer technique. Advanced Materials (Deerfield Beach, Fla.), 2011, 23 (24): 2764–2768
16. Huang F Z, Chen D H, Cao L, Caruso R A, Cheng Y B. Flexible dye-sensitized solar cells containing multiple dyes in discrete layers. Energy & Environmental Science, 2011, 4(8): 2803–2806
17. Murayama M, Mori T. Dye-sensitized solar cell using novel tandem cell structure. Journal of Physics D, Applied Physics, 2007, 40(6): 1664–1668
18. Murayama M, Mori T. Novel tandem cell structure of dye-sensitized solar cell for improvement in photocurrent. Thin Solid Films, 2008, 516(9): 2716–2722
19. Kenshiro U, Shyam S P, Shuzi H. Tandem dye-sensitized solar cells consisting of floating electrode in one cell. Journal of Photochemistry and Photobiology A, Chemistry, 2010, 216(2–3): 104–109
20. He J, Lindström H, Hagfeldt A, Lindquist S. Dye-sensitized nanostructured p-type nickel oxide film as a photocathode for a solar cell. Journal of Physical Chemistry B, 1999, 103(42): 8940–8943
21. Powar S, Wu Q, Weidelener M, Nattesta A, Hu Z, Mishra A, Bauerle P, Spiccia L, Cheng Y B, Bach U. Improved photocurrents for p-type dye-sensitized solar cells using nano-structured nickel(II) oxide microballs. Energy & Environmental Science, 2012, doi: 10.1039/C2EE22127F
22. He J, Lindström H, Hagfeldt A, Lindquist S E. Dye-sensitized nanostructured tandem cell first demonstrated cell with a dye-sensitized photocathode. Solar Energy Materials and Solar Cells, 2000, 62(3): 265–273
23. Nakasa A, Usami H, Sumikura S, Hasegawa S, Koyama T, Suzuki E. A high voltage dye-sensitized solar cell using a nanoporous NiO photocathode. Chemistry Letters, 2005, 34(4): 500–501
24. Nattestad A, Ferguson M, Kerr R, Cheng Y B, Bach U. Dye-sensitized nickel(II)oxide photocathodes for tandem solar cell applications. Nanotechnology, 2008, 19(29): 295304
25. Mizoguchi Y, Fujihara S. Fabrication and dye-sensitized solar cell performance of nanostructured NiO/Coumarin 343 photocathodes. Electrochemical and Solid-State Letters, 2008, 11(8): K78–K80
26. Qin P, Zhu H, Edvinsson T, Boschloo G, Hagfeldt A, Sun L C. Design of an organic chromophore for p-type dye-sensitized solar cells. Journal of the American Chemical Society, 2008, 130(27): 8570–8571
27. Mori S, Fukuda S, Sumikura S, Takeda Y, Tamaki Y, Suzuki E, Abe T. Charge-transfer processes in dye-sensitized NiO solar cells. Journal of Physical Chemistry C, 2008, 112(41): 16134–16139
28. Lepleux L, Chavillon B, Pellegrin Y, Blart E, Cario L, Jobic S, Odobel F. Simple and reproducible procedure to prepare self-nanostructured NiO films for the fabrication of p-type dye-sensitized solar cells. Inorganic Chemistry, 2009, 48(17): 8245–8250
29. Qin P, Linder M, Brinck T, Boschloo G, Hagfeldt A, Sun L C. High incident photon-to-current conversion efficiency of p-type dye-sen sitized solar cells based on NiO and organic chromophores. Advanced Materials (Deerfield Beach, Fla.), 2009, 21(29): 2993–2996
30. Gibson E A, Smeigh A L, Le Pleux L, Fortage J, Boschloo G, Blart E, Pellegrin Y, Odobel F, Hagfeldt A, Hammarström L. A p-type NiO-based dye-sensitized solar cell with an open-circuit voltage of 0.35 V. Angewandte Chemie International Edition, 2009, 48(24): 4402–4405
31. Li L, Gibson E A, Qin P, Boschloo G, Gorlov M, Hagfeldt A, Sun L C. Double-layered NiO photocathodes for p-type DSSCs with record IPCE. Advanced Materials (Deerfield Beach, Fla.), 2010, 22 (15): 1759–1762
32. Qin P, Wiberg J, Gibson E A, Linder M, Li L, Brinck T, Hagfeldt A, Albinsson B, Sun L C. Synthesis and mechanistic studies of organic chromophores with different energy levels for p-type dye-sensitized solar cells. Journal of Physical Chemistry C, 2010, 114(10): 4738–4748
33. Nattestad A, Mozer A J, Fischer M K R, Cheng Y B, Mishra A, Bäuerle P, Bach U. Highly efficient photocathodes for dye-sensitized tandem solar cells. Nature Materials, 2010, 9(1): 31–35
34. Zhang X L, Huang F, Nattestad A, Wang K, Fu D, Mishra A, Bäuerle P, Bach U, Cheng Y B. Enhanced open-circuit voltage of p-type DSC with highly crystalline NiO nanoparticles. Chemical Communications, 2011, 47(16): 4808–4810
35. Zhang X L, Zhang Z, Huang F, Bäuerle P, Bach U, Cheng Y B. Charge transport in photocathodes based on the sensitization of NiO Nanorods. Journal of Materials Chemistry, 2012, 22(14): 7005–7009
36. Ji Z Q, Natu G, Huang Z J, Wu Y Y. Linker effect in organic donor-acceptor dyes for p-type NiO dye sensitized solar cells. Energy &Environmental Science, 2011, 4(8): 2818–2821
37. Ji Z Q, Natu G, Huang Z J, Kokhan O, Zhang X Y, Wu Y Y. Synthesis, photophysics and photovoltaic studies of ruthenium cyclometalated complexes as sensitizers for p-type NiO dye-sensitized solar cells. Journal of Physical Chemistry C, 2012, 116 (32): 16854–16863
38. Pellegrin Y, Pleux L, Blart E, Renaud A, Chavillon B, Szuwarski N, Boujtita M, Cario L, Jobic S, Jacquemin D, Odobel F. Ruthenium polypyridine complexes as sensitizers in NiO based p-type dye-sensitized solar cells: effects of the anchoring groups. Journal of Photochemistry and Photobiology A, Chemistry, 2011, 219(2–3): 235–242
39. Gibson E A, Smeigh A L, Le Pleux L, Hammarström L, Odobel F, Boschloo G, Hagfeldt A. Cobalt polypyridyl-based electrolytes for p-type dye-sensitized solar cells. Journal of Physical Chemistry C, 2011, 115(19): 9772–9779
40. Nattestad A, Zhang X, Bach U, Cheng Y B. Dye-sensitized $CuAlO_2$ photocathodes for tandem solar cell applications. Journal of

Photonics for Energy, 2011, 1(1): 011103
41. Yu M Z, Natu G, Ji Z Q, Wu Y Y. p-type dye-sensitized solar cells based on delafossite $CuGaO_2$ nanoplates with saturation photovoltages exceeding 460 mV. Journal of Physical Chemistry Letters, 2012, 3(9): 1074–1078
42. Renaud A, Chavillon B, Le Pleux L, Pellegrin Y, Blart E, Boujtita M, Pauporté T, Cario L, Jobic S, Odobel F. $CuGaO_2$ a promising alternative for NiO in p-type dye solar cells. Journal of Materials Chemistry, 2012, 22(29): 14353–14356
43. Nakabayashi S, Ohta N, Fujishima A. Dye sensitization of synthetic p-type diamond electrode. Physical Chemistry Chemical Physics, 1999, 1(17): 3993–3997
44. Sumikura S, Mori S, Shimizu S, Usami H, Suzuki E. Photoelectrochemical characteristics of cells with dyed and undyed nanoporous p-type semiconductor CuO electrodes. Journal of Photochemistry and Photobiology A, Chemistry, 2008, 194(2–3): 143–147
45. Chitambar M, Wang Z, Liu Y, Rockett A, Maldonado S. Dye-sensitized photocathodes: efficient light-stimulated hole injection into p-GaP under depletion conditions. Journal of the American Chemical Society, 2012, 134(25): 10670–10681
46. Vera F, Schrebler R, Munoz E, Suarez C, Cury P, Gomez H, Cordova R, Marotti R E, Dalchiele E A. Preparation and characterization of eosin B- and erythrosin J-sensitized nanostructured NiO thin film photocathodes. Thin Solid Films, 2005, 490(2): 182–188
47. Xi Y Y, Li D, Djurišić A B, Xie M H, Man K Y K, Chan W K. Hydrothermal synthesis vs electrodeposition for high specific capacitance nanostructured NiO films. Electrochemical and Solid-State Letters, 2008, 11(6): D56–D59
48. Zhu H, Hagfeldt A, Boschloo G. Photoelectrochemistry of mesoporous NiO electrodes in iodide/triiodide electrolytes. Journal of Physical Chemistry C, 2007, 111(47): 17455–17458
49. Uehara S, Sumikura S, Suzuki E, Mori S. Retardation of electron injection at NiO/dye/electrolyte interface by aluminium alkoxide treatment. Energy & Environmental Science, 2010, 3(5): 641–644
50. Bian Z, Tachikawa T, Cui S C, Fujitsuka M, Majima T. Single-molecule charge transfer dynamics in dye-sensitized p-type NiO solar cells: influences of insulating Al_2O_3 Layers. Chemical Science, 2012, 3(2): 370–379
51. Nagarajan R, Draeseke A D, Sleight A W, Tate J. p-type conductivity in $CuCr_{1-x}Mg_xO_2$ films and powders. Journal of Applied Physics, 2001, 89(12): 8022–8025
52. Gillen R, Robertson J. Band structure calculations of $CuAlO_2$, $CuGaO_2$, $CuInO_2$ and $CuCrO_2$ by screened exchange. Physical Review B: Condensed Matter and Materials Physics, 2011, 84(3): 035125
53. Morandeira A, Boschloo G, Hagfeldt A, Hammarström L. Photoinduced ultrafast dynamics of coumarin 343 sensitized p-type-nanostructured NiO films. Journal of Physical Chemistry B, 2005, 109(41): 19403–19410
54. Rehm J, McLendon G, Nagasawa Y, Yoshihara K, Moser J, Grätzel M. Femtosecond electron-transfer dynamics at a sensitizing dye-semiconductor (TiO_2) interface. Journal of Physical Chemistry, 1996, 100(23): 9577–9578
55. Borgström M, Blart E, Boschloo G, Mukhtar E, Hagfeldt A, Hammarström L, Odobel F. Sensitized hole injection of phosphorus porphyrin into NiO: toward new photovoltaic devices. Journal of Physical Chemistry B, 2005, 109(48): 22928–22934
56. Sánchez-de-Armas R, San Miguel M Á, Oviedo J, Sanz J F. Coumarin derivatives for dye sensitized solar cells: a TD-DFT study. Physical Chemistry Chemical Physics, 2012, 14(1): 225–233
57. Morandeira A, Fortage J, Edvinsson T, Le Pleux L, Blart E, Boschloo G, Hagfeldt A, Hammarström L, Odobel F. Improved photon-to-current conversion efficiency with a nanoporous p-type NiO electrode by the use of a sensitizer-acceptor dyad. Journal of Physical Chemistry C, 2008, 112(5): 1721–1728
58. Eggeling C, Ringemann C, Medda R, Schwarzmann G, Sandhoff K, Polyakova S, Belov V N, Hein B, von Middendorff C, Schönle A, Hell S W. Direct observation of the nanoscale dynamics of membrane lipids in a living cell. Nature, 2009, 457(7233): 1159–1162
59. Wu X, Xing G, Tan S L, Webster R D, Sum T C, Yeow E K. Hole transfer dynamics from dye molecules to p-type NiO nanoparticles: effects of processing conditions. Physical Chemistry Chemical Physics, 2012, 14(26): 9511–9519
60. Morandeira A, Boschloo G, Hagfeldt A, Hammarström L. Coumarin 343-NiO films as nanostructured photocathodes in dye-sensitized solar cells: ultrafast electron transfer, effect of the I_3^-/I^- Redox couple and mechanism of photocurrent generation. Journal of Physical Chemistry C, 2008, 112(25): 9530–9537
61. Bremner S P, Levy M Y, Honsberg C B. Analysis of tandem solar cell efficiencies under AM1.5G spectrum using a rapid flux calculation method. Progress in Photovoltaics: Research and Applications, 2008, 16(3): 225–233
62. Liska P, Thampi K R, Grätzel M, Brémaud D, Rudmann D, Upadhyaya H M, Tiwari A N. Nanocrystalline dye-sensitized solar cell/copper indium gallium selenide thin-film tandem showing greater than 15% conversion efficiency. Applied Physics Letters, 2006, 88(20): 203103
63. Wang W L, Lin H, Zhang J, Li X, Yamada A, Konagai M, Li J B. Experimental and simulation analysis of the dye sensitized solar cell/Cu(In,Ga)Se_2 solar cell tandem structure. Solar Energy Materials and Solar Cells, 2010, 94(10): 1753–1758
64. Jeong W S, Lee J W, Jung S, Yun J H, Park N G. Evaluation of external quantum efficiency of a 12.35% tandem solar cell comprising dye-sensitized and CIGS solar cells. Solar Energy Materials and Solar Cells, 2011, 95(12): 3419–3423
65. Ito S, Dharmadasa I M, Tolan G J, Roberts J S, Hill G, Miura H, Yum J H, Pechy P, Liska P, Comte P, Grätzel M. High-voltage (1.8 V) tandem solar cell system using a GaAs/$Al_xGa_{(1-x)}$ As graded solar cell and dye-sensitised solar cells with organic dyes having different absorption spectra. Solar Energy, 2011, 85(6): 1220–1225
66. Greg D B, Paul G H, Seung-Hyun A L, Neal M A, Janine M, Thomas E M, Paul L, Shaik M Z, Michael G, Anita H B, Martin A G. Utilization of direct and diffuse sunlight in a dye-sensitized solar cell-silicon photovoltaic hybrid concentrator system. Journal of Physical Chemistry Letters, 2011, 2(6): 581–585
67. Ingmar B, Martin K, Felix E, Jaehyung H, Peter E, Anders H, Jürgen W, Neil P. Efficient organic tandem cell combining a solid state dye-sensitized and a vacuum deposited bulk heterojunction solar cell. Solar Energy Materials and Solar Cells, 2009, 93(10): 1896–1899

68. Guo X Z, Zhang Y D, Qin D, Luo Y H, Li D M, Pang Y T, Meng Q B. Hybrid tandem solar cell for concurrently converting light and heat energy with utilization of full solar spectrum. Journal of Power Sources, 2010, 195(22): 7684–7690
69. Wang N, Han L, He H C, Park N H, Koumoto K. A novel high-performance photovoltaic-thermoelectric hybrid device. Energy & Environmental Science, 2011, 4(9): 3676–3679
70. Jeremie B, Maurin C, Florian L, Jun-Ho Y, Michael G, Kevin S. Examining architectures of photoanode-photovoltaic tandem cells for solar water splitting. Journal of Materials Research, 2010, 25(1): 17–24
71. Kim J K, Shin K, Cho Sung M, Lee T W, Park J H. Synthesis of transparent mesoporous tungsten trioxide films with enhanced photoelectrochemical response: application to unassisted solar water splitting. Energy & Environmental Science, 2011, 4(4): 1465–1470